Ultrahigh-energy neutrino events in current and future neutrino telescopes from nearby Gamma-Ray Bursts

Jessymol K Thomas, Reetanjali Moharana and Soebur Razzaque

Department of Physics, University of Johannesburg, P.O. Box 524, Auckland Park 2006, South Africa.

E-mail: jessymolkt@uj.ac.za

Abstract. Neutrino Astronomy has gained momentum after discovering cosmic neutrinos by the IceCube Neutrino Observatory at the south pole. A proposed upgrade of IceCube and planned future experiments will increase sensitivity to neutrino fluxes at very high energies ($>$ PeV). We consider very high-energy neutrino flux from the Gamma Ray Bursts (GRBs) during the afterglow phase. We calculate this flux by modeling in details the observed afterglow data with standard afterglow theories for nearby long-duration GRBs within redshift 0.5. We also calculate neutrino events and corresponding upper limits from these GRBs for the future IceCube Gen-2 observatory.

1. Introduction

Gamma ray bursts are one of the most energetic transients and they have been proposed as sources of very high energy neutrinos. Ultra High Energy Cosmic Rays (UHECRs) are expected to be produced from shock acceleration in GRBs. These UHECRs can interact with low energy afterglow photons to produce very high energy neutrinos [1, 2]. We have modeled afterglow radiations of 17 nearby GRBs within redshift 0.5, and using the best fitted afterglow model parameters we have calculated expected neutrino flux and events from them. The synchrotron modeling of broadband spectral energy distribution (SED) at different time intervals and the temporal evolution of flux in different frequencies are done for all the 17 GRBs, using theories of blast wave evolution in the constant density interstellar medium (ISM) and in wind environment where the density decreases with distance from the center of the GRB (here after called as wind medium).

The high energy neutrino observatories such as IceCube, have recently successfully demonstrated the existence of astrophysical neutrino flux and this result is one of the driving consideration for the second generation detector at south pole, the IceCube-Gen-2 [3]. We have calculated neutrino fluence from individual GRBs in our sample, and by stacking fluence from all GRBs we have calculated neutrino events for the upcoming IceCube Gen-2 in both ISM and wind environment. We have also calculated upper limits for the stacked fluence of the IceCube Gen-2 observatory since no detection seems to be possible.

2. Synchrotron modeling of GRB afterglow

In the GRB explosions the afterglows follow the prompt emissions ($<$ 2 s for short GRBs and $>$ 2 s for long GRBs) and are produced by the synchrotron emission of accelerated electrons in

the GRB blastwave [4, 5]. Relativistic material ejected from GRB explosion drives a blastwave by accumulating surrounding medium. As the shock front propagates in the blast wave, a population of electrons gets accelerated to relativistic energies by a Fermi shock-acceleration mechanism. These electrons emit synchrotron radiations in a random magnetic field created (assuming some plasma instability) in the shock region. This synchrotron radiation is observed afterglows in all electromagnetic wavelengths. The synchrotron modeling of an afterglow spectrum is done for a power-law distribution of electrons with Lorentz factors γ as $n_e(\gamma) \propto \gamma^{-p}$ in the range $\gamma_{min} \leq \gamma \leq \gamma_s$. Here γ_{min} and γ_s are the minimum and maximum Lorentz factors, respectively and p the spectral index. Several breaks can appear in the electron spectrum due to efficient synchrotron cooling at high energies (γ_c) and synchrotron self-absorption at low energies. These breaks also give rise to breaks in the synchrotron spectrum, in the so-called slow-cooling ($\gamma_c > \gamma_{min}$) and fast-cooling regime ($\gamma_c < \gamma_{min}$) [5, 6, 7].

We have used afterglow data from gamma-ray to optical range which are detected by the Large Area Telescope (LAT) on board the Fermi Gamma ray Space Telescope, the Burst Alert Telescope (BAT),the X-ray Telescope (XRT) and the Ultraviolet/Optical Telescope (UVOT) of the Swift Gamma Ray Burst explorer and the data observed by other optical telescopes. The SEDs are taken for different time intervals from early time after T_{90} (duration of GRB prompt phase) to later times depending on the availability of data. The synchrotron modeling of the observed photon fluxes for the 17 GRB afterglows are done for both the ISM and wind media. We show in Fig. 1 and Fig. 2, as examples, the SEDs and light curves for GRB 150818A in the wind environment. Note that the blast wave model cannot explain well the light curve in Fig. 2 during the 100-500 s period, which reflects our still inadequate understanding of the afterglow emission models.

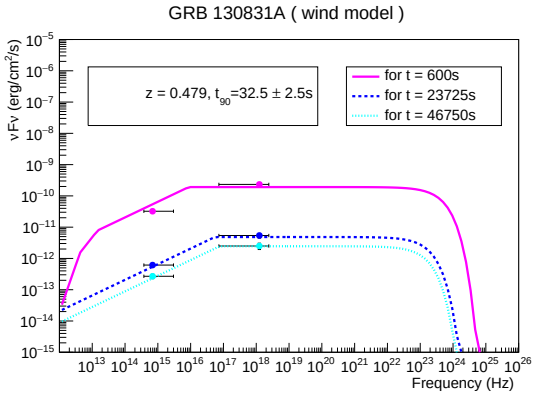

Figure 1. SEDs for GRB 130831A in wind medium at different times after T_{90}.

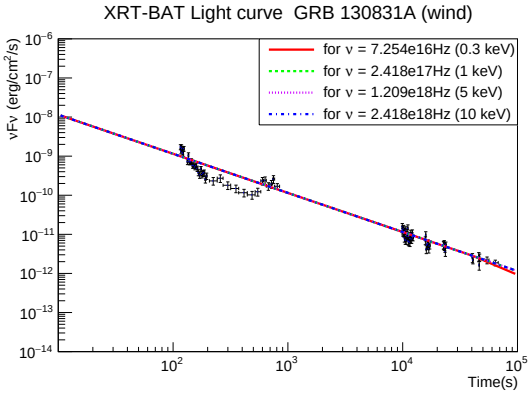

Figure 2. Swift-XRT light curves for GRB 130831A at different frequencies.

We have listed afterglow model parameters from our fits to 17 GRBs in Table 1 for the wind environment and in Table 2 for ISM. In these tables, E_{iso} is the isotropic-equivalent radiated gamma-ray energy within T_{90}, $E_{kin}(10^{55}\ erg)$ is the initial kinetic energy of the GRB blast wave in units of 10^{55} ergs, ϵ_e is the fraction of shock energy going to the relativistic electrons, ϵ_b is the fraction of shock energy going to the magnetic energy, $A_* \equiv \dot{M}_{-5}/v_8$, corresponding to a mass-loss rate of $\dot{M}_w = 10^{-5}\dot{M}_{-5}M_\odot \mathrm{yr}^{-1}$ in wind, with velocity $v_w = 10^8 v_8$ cms^{-1}, by the progenitor star and n_0 is the number density of particles in the ISM.

3. Neutrino flux and events from GRBs

We have used the above modeled parameters for the afterglow radiation to calculate the neutrino flux and events from the GRBs by the upcoming IceCube Gen-2 neutrino telescope. In GRB

Table 1. WIND Model parameters

GRB	z	$T_{90}(s)$	$E_{iso}(erg)$	$E_{kin}(10^{55}erg)$	ϵ_e	ϵ_b	p	$A*$
150818A	0.282	123.3±31.3	1×10^{51}	1×10^{-3}	6×10^{-3}	1×10^{-2}	2.14	0.1
130831A	0.479	32.5 ± 2.5	4.56×10^{51}	8×10^{-3}	9×10^{-3}	1×10^{-3}	2.0	1.0
130702A	0.145	15±1	7.8×10^{50}	7×10^{-4}	2×10^{-2}	5×10^{-2}	1.9	0.1
130427A	0.34	162.83±1.36	8.5×10^{53}	1.1	9×10^{-3}	1×10^{-4}	2.0	1.0
120714B	0.398	159 ± 34	4.51×10^{51}	4.5×10^{-3}	1×10^{-2}	1.2×10^{-3}	2.3	0.1
120422A	0.28	5.35±1.4	1.28×10^{51}	1.28×10^{-3}	3.5×10^{-2}	1×10^{-4}	2.4	1.0
111225A	0.297	106.8±26.7	2.88×10^{50}	2.88×10^{-4}	1×10^{-2}	1.45×10^{-2}	2.18	0.1
100316D	0.059	1300	9.81×10^{48}	9.8×10^{-6}	8×10^{-3}	1×10^{-4}	2.12	0.1
091127	0.49	7.1±0.2	1.60×10^{52}	1.6×10^{-2}	3×10^{-2}	5×10^{-3}	2.0	0.1
061021	0.346	46	4.06×10^{51}	4.06×10^{-3}	6×10^{-3}	4×10^{-3}	2.0	0.1
060614	0.125	102	8.4×10^{50}	8.4×10^{-4}	3×10^{-3}	2×10^{-3}	2.1	0.1
060512	0.443	8.6± 2	1.99×10^{50}	1.99×10^{-4}	5×10^{-2}	1×10^{-2}	2.18	0.1
060218	0.033	2100± 0.1	1.9×10^{49}	1.9×10^{-5}	1×10^{-2}	6.8×10^{-2}	2.27	0.1
051117B	0.481	8	2.77×10^{51}	2.77×10^{-3}	2×10^{-3}	3×10^{-4}	2.1	0.1
051109B	0.08	151	3.46×10^{48}	3.4×10^{-6}	2×10^{-2}	1×10^{-3}	2.0	0.1
050826	0.297	35± 8	3.39×10^{50}	3.39×10^{-4}	1×10^{-2}	5×10^{-3}	2.12	0.1
050803	0.422	85 ± 10	2.45×10^{51}	2.45×10^{-3}	2×10^{-2}	1×10^{-3}	2.0	0.1

Table 2. ISM Model parameters

GRB	z	$T_{90}(s)$	$E_{iso}(erg)$	$E_{kin}(10^{55}erg)$	ϵ_e	ϵ_b	p	n_0
150818A	0.282	123.3± 31.3	1×10^{51}	1×10^{-3}	1×10^{-3}	1×10^{-2}	2.02	1
130831A	0.479	32.5 ± 2.5	4.56×10^{51}	8×10^{-3}	3×10^{-3}	1×10^{-1}	2.0	0.01
130702A	0.145	15±1	7.8×10^{50}	7×10^{-4}	$5\times10^{-}3$	8×10^{-2}	1.87	0.1
130427A	0.34	162.83±1.36	8.5×10^{53}	5×10^{-1}	1.2×10^{-3}	1×10^{-4}	2.0	1.0
120714B	0.398	159 ± 34	4.51×10^{51}	4.5×10^{-3}	2×10^{-3}	2×10^{-3}	2.28	1.0
120422A	0.28	5.35±1.4	1.28×10^{51}	1.28×10^{-3}	1×10^{-3}	1.3×10^{-2}	2.1	1.0
111225A	0.297	106.8±26.7	2.88×10^{50}	2.88×10^{-4}	4.5×10^{-3}	1.6×10^{-2}	2.19	1.0
100316D	0.059	1300	9.81×10^{48}	9.8×10^{-6}	1×10^{-3}	1×10^{-3}	2.12	0.1
091127	0.49	7.1±0.2	1.60×10^{52}	1.6×10^{-2}	1.2×10^{-2}	3.8×10^{-3}	2.0	0.1
061021	0.346	46±1	4.06×10^{51}	4.06×10^{-3}	4×10^{-3}	3×10^{-3}	2.0	0.1
060614	0.125	102	8.4×10^{50}	8.4×10^{-4}	2×10^{-3}	2×10^{-3}	2.18	1.0
060512	0.443	8.6± 2	1.99×10^{50}	1.99×10^{-4}	2×10^{-2}	3×10^{-2}	2.18	1.0
060218	0.033	2100	1.9×10^{49}	1.9×10^{-5}	1×10^{-2}	2×10^{-2}	2.27	0.14
051117B	0.481	8	2.77×10^{51}	2.77×10^{-3}	5×10^{-4}	1×10^{-3}	2.0	1.0
051109B	0.08	151	3.46×10^{48}	3.4×10^{-6}	2×10^{-2}	3×10^{-2}	2.1	1.0
050826	0.297	35±8	3.39×10^{50}	3.39×10^{-4}	4×10^{-3}	1×10^{-2}	2.14	1.0
050803	0.422	85±10	2.45×10^{51}	2.45×10^{-3}	7×10^{-3}	1×10^{-3}	2.0	1.0

blast waves, the low energy afterglow photons interacts with the UHECRs to produce muons, pions and kaons. Subsequently they decay to produce very high energy neutrinos. Due to neutrino oscillation during their propagation we expect 3 different neutrino flavors: muon neutrino, electron neutrino and tau neutrino and their anti neutrinos on the Earth. Here we have calculated the neutrino flux from pion and muon decay considering their production from Δ^+ resonance interaction $p\gamma \rightarrow \Delta^+ \rightarrow n\pi^+$ or $p\pi^0$, where n is neutron and p is proton. Subsequent decay channels for neutrino production are $\pi^+ \rightarrow \mu^+ + \nu_\mu \rightarrow e^+ + \nu_e + \nu_\mu + \bar{\nu}_\mu$.

3.1. Neutrino flux from GRBs

Using the synchrotron model parameters from the 17 GRBs we have modeled neutrino flux for all of them individually for different time intervals in terms of T_{90}. The neutrino flux from the proton-photon ($p\gamma$) interactions depends on the proper density of synchrotron photons in the blast wave frame and corresponding optical depth (efficiency) and the flux of cosmic-ray protons from the GRB blast wave. The photon spectrum in the blast wave can be expressed in terms of the differential proper density of the synchrotron photon $n'_\gamma(E'_\gamma)$ in the slow-cooling and fast-cooling regime [5, 1]. Here E'_γ is the photon energy in the blast wave frame and it is related to the observed synchrotron photon energy $h\nu$ as $E'_\gamma = h\nu(1+z)/\Gamma$, where Γ is the bulk Lorentz factor of the blast wave. The $p\gamma$ optical depth is $\tau_{p\gamma}(E'_\gamma) \approx E' n'_\gamma(E')\sigma_{p\gamma} c t_{dyn}$, where t_{dyn} is the dynamic time. The optical depth as a function of the photon energy E'_γ can be converted to a function of the proton energy E'_p in the blast wave frame using the resonance energy for $p\gamma \rightarrow \Delta^+$ production as $E'_\gamma E'_p = 0.3$ GeV^2. In the observer's frame $E_p = E'_p(1+z)/\Gamma$.

The $p\gamma$ opacity scales with the proton energy E_p in the slow-cooling regime as [9]

$$\tau_{p\gamma}(E_p) = \tau_{p\gamma}(E_{pl}) \times \begin{cases} (\frac{E_{ph}}{E_{pl}})^{\frac{p}{2}-\frac{1}{2}} (\frac{E_p}{E'_{Ph}})^{\frac{p}{2}}; \ E_p < E_{ph}, \\ (\frac{E_p}{E_{pl}})^{\frac{p}{2}-\frac{1}{2}}; \ E_{ph} < E_p < E_{pl}, \\ 1; \ E_p > E_{pl}. \end{cases} \quad (1)$$

and in the fast-cooling regime as

$$\tau_{p\gamma}(E_p) = \tau_{p\gamma}(E_{pl}) \times \begin{cases} (\frac{E_p}{E_{pl}})^{p/2}; \ E_p < E_{pl}, \\ (\frac{E_p}{E_{pl}})^{1/2}; \ E_{pl} < E_p < E_{ph}, \\ (\frac{E_{ph}}{E_{pl}})^{1/2}; \ E_p > E_{ph}. \end{cases} \quad (2)$$

Here E_{pl} is the minimum proton energy corresponding to the break energy $h\nu_m$ in the afterglow synchrotron photon spectrum, corresponding to the electrons with minimum Lorentz factor γ_{min}. Similarly E_{ph} is the proton energy corresponding to the break energy $h\nu_c$ in the afterglow synchrotron photon spectrum, corresponding to the electrons with the cooling Lorentz factor γ_c. We refer the readers for details in [1] for equations and numerical values for these energies. The opacity value at the energy E_{pl} in the wind medium is,

$$\tau_{p\gamma}(E_{pl}) = 6.0(1+z)^{1/2} \epsilon_{b,0.1}^{1/2} A_*^2 t_2^{-1/2} E_{55}^{-1/2}, \quad (3)$$

where $t_2 = t/100$ and t is the time after the prompt emission. Similarly the opacity value at the energy E_{pl} for ISM is calculated as,

$$\tau_{p\gamma}(E_{pl}) = 0.7(1+z)^{-1/2} \epsilon_{b,0.1}^{1/2} n_0 t_2^{1/2} E_{55}^{1/2}. \quad (4)$$

The neutrino flux from the GRB afterglow is calculated from shock-accelerated cosmic-rays interacting with afterglow synchrotron photons as described above. We assume that cosmic-ray is dominated by protons and for calculation purpose we use a primary cosmic-ray flux and a pion flux, although those cannot escape directly the blast wave. The cosmic-ray spectrum, $n(E_p)$ or dN/dE, is a power-law of energy with index -2, assumed to originate from Fermi acceleration. The normalization of the spectrum is done by integrating the differential spectrum $E(dN/dE)$ over the minimum and maximum energy range of protons and equating it to the total kinetic energy (dominated by protons) of the GRB blast wave [1]. The proton flux and is given as $J_P(E_p) = c/4\pi(R/d_l)^2 n(E_p)$, where d_l is the luminosity distance of the GRB. An intermediate pion flux, from $p\gamma$ interactions, can be calculated as $J_\pi(E_\pi) = J_p(E_p)\tau_{p\gamma}(E_p) f_{p\rightarrow\pi}(x)$, where $x = E_\pi/E_p$ and we took the average value of x as 0.2. We have calculated neutrino flux by assuming an average of $1/4^{th}$ energy of pion goes to one neutrino.

The neutrino flux for individual GRBs at time T_{90} for the ISM and wind environment are shown in Fig. 3 and Fig. 4, respectively and at $100\,T_{90}$ for the ISM and wind environment are shown in Fig. 5 and Fig. 6, respectively.

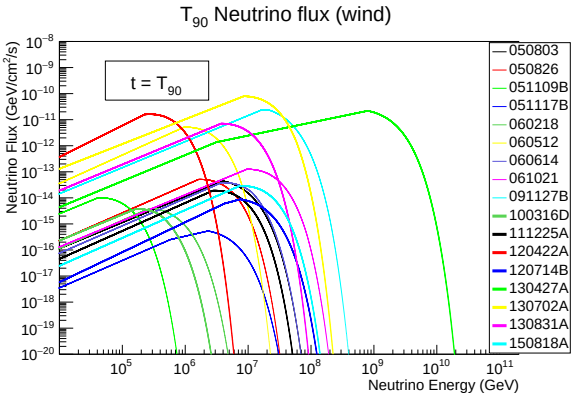

Figure 3. Neutrino flux calculated for T_{90} in the wind environment.

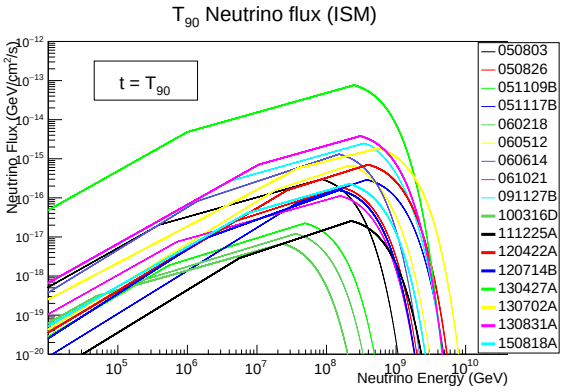

Figure 4. Neutrino flux calculated for T_{90} in the ISM.

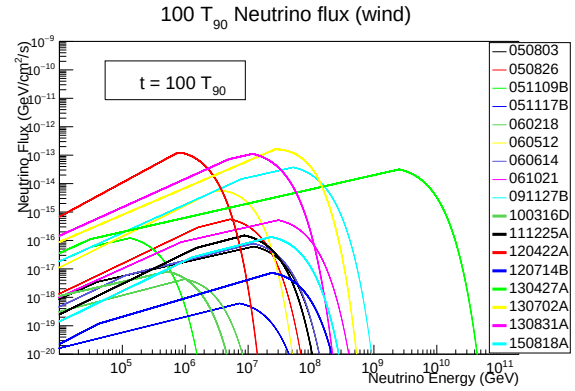

Figure 5. Neutrino flux calculated for $100\,T_{90}$ in the wind environment.

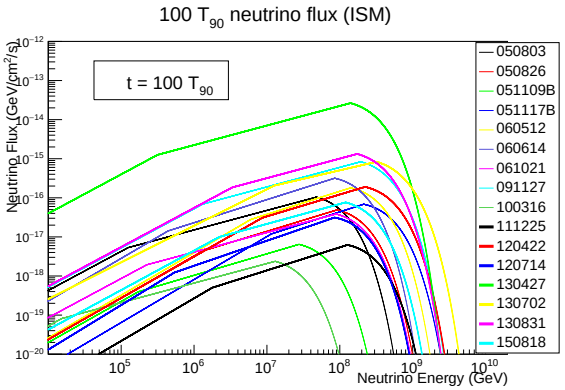

Figure 6. Neutrino flux calculated for $100\,T_{90}$ in the ISM.

3.2. Neutrino events and fluence upper limit calculated for the IceCube Gen-2 .
The Neutrino observatories have made a significant progress in the study and research of Astrophysical Neutrinos. Out of the modeled 17 nearby long GRBs we have calculated the neutrino events and individual fluence from the 7 southern hemisphere GRBs which could be in the field of view of IceCube Gen-2. We also have stacked the fluence of all these 7 GRBs. Figures 7 and 8 show the neutrino fluence plots of the southern hemisphere GRBs for the IceCube Gen-2 in ISM and wind environment, respectively. In case of non-detection of neutrinos, the upper limits for the stacked fluence is also calculated. We calculated the neutrino events as,

$$N_\nu = \int_{E_{\nu,min}}^{E_{\nu,max}} \int_{T_{90}}^{100T_{90}} \frac{dN_\nu}{dE_\nu} A_{eff} dE_\nu dt_{90}, \tag{5}$$

where A_{eff} is the effective area for the IceCube Gen-2 [3], $E_{\nu,min} = 10^6$ GeV and $E_{\nu,max} = 10^9$ GeV. These upper limits on the stacked fluence for the 7 GRBs are also shown in Figs. 7 and 8.

Estimated neutrino fluence for IceCube corresponding to 468 long GRBs detected within 4 years (2011-2015) has been reported in Ref. [11], which gives an upper limit on the flux as $\approx 10^{-4}$ GeV cm^{-2} sr^{-1}. This calculation considers both prompt and afterglow neutrino production in GRBs. Again IceCube Gen-2 has atleast one order of magnitude larger effective

area compared to IceCube [12]. Hence we have not done a precise nuetrino event calculation for IceCube.

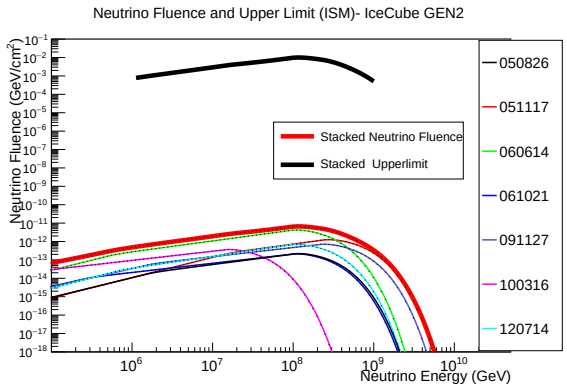

Figure 7. Neutrino fluence and upper limit calculated from time T_{90} to $100\,T_{90}$ for IceCube Gen-2 in ISM.

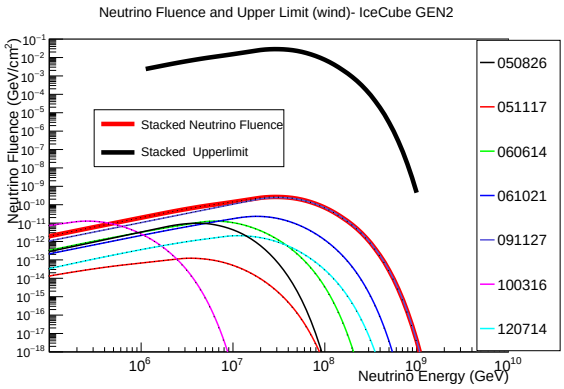

Figure 8. Neutrino fluence and upper limit from T_{90} to $100\,T_{90}$ for IceCube Gen-2 in wind medium.

4. Discussion and conclusion

We have done a detailed study of afterglow radiations from a well defined set of 17 long nearby GRBs with redshift less than 0.5, which are the most promising GRBs for the neutrino detection. We have modeled the SED for different time intervals and the light curves for different frequencies of the afterglows of these GRBs. For this afterglow modeling we have used different data from LAT, XRT/BAT, UVOT/optical and other optical telescopes. We have obtained a set of reasonable model parameters for all these GRBs in both the constant density interstellar medium and wind environment.

We have calculated neutrino flux and fluence from the southern hemisphere GRBs for the IceCube Gen-2 neutrino observatory. Individual fluences for the 7 southern hemisphere GRBs are calculated and the stacked fluence of these GRBs are calculated. The number of neutrino events for the stacked fluence is very small and in such a case of non-detection we have calculated upper limit for these stacked fluences. Our calculations are useful to estimate sensitivity of new generation of neutrino telescopes for detecting very high energy (> 1 PeV) neutrinos from the afterglows of long-durations GRBs.

5. References

[1] Razzaque S 2013, *Phys. Rev.* D **88** 103003
[2] Waxman E and Bahcall J N 1997, *Phys. Rev. Lett.* **78** 2292
[3] Aartsen, M G et al 2015, *PoS(ICRC2015)* 1148
[4] Meszaros P and Rees M J 1997, *Astrophys.J.* **476** 23
[5] Piran T 2005, *Rev. Mod. Phys.* **76** 1143
[6] Thomas J, Moharana R, Razzaque S 2015, *Pos(HEASA2015)* 038
[7] Thomas J, Moharana R, Razzaque S 2015, *Pos(SSC2015)* 073
[8] Thomas J, Moharana R, Razzaque S 2015, *Pos(SAIP2015)*
[9] Razzaque S, Yang L 2015, *Phys.Rev.* D **91** 043003
[10] Hanson K 2015, *in VLVnT Workshop in La Sapienza (Rome, Italy)*
[11] Brayeur L, 2015 Thesis, *https://inspirehep.net/record/1513509/files/LionelBrayeur-PhD-thesis.pdf*
[12] Halzen F 2015, *in 25th International Workshop on Weak Interactions and Neutrinos (Heidelberg, Germany)*